

# Zhiqing Zhang

## List of Publications by Year in descending order

Source: <https://exaly.com/author-pdf/6153888/publications.pdf>

Version: 2024-02-01

106  
papers

9,833  
citations

53660

45  
h-index

33814

99  
g-index

108  
all docs

108  
docs citations

108  
times ranked

7917  
citing authors

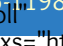
#	ARTICLE	IF	CITATIONS
1	The anomalous magnetic moment of the muon in the Standard Model. <i>Physics Reports</i> , 2020, 887, 1-166.	10.3	790
2	Reevaluation of the hadronic contributions to the muon $g-2$ and to $\alpha(M_Z^2)$ . <i>European Physical Journal C</i> , 2011, 71, 1.	1.4	628
3	Performance of the ATLAS trigger system in 2015. <i>European Physical Journal C</i> , 2017, 77, 317.	1.4	489
4	Combined measurement and QCD analysis of the inclusive $e^\pm p$ scattering cross sections at HERA. <i>Journal of High Energy Physics</i> , 2010, 2010, 1.	1.6	458
5	Muon reconstruction performance of the ATLAS detector in proton-proton collision data at $\sqrt{s} = 13$ TeV. <i>European Physical Journal C</i> , 2016, 76, 292.	1.4	453
6	Reevaluation of the hadronic vacuum polarisation contributions to the Standard Model predictions of the muon $g-2$ and $\alpha(m_Z^2)$ using newest hadronic cross-section data. <i>European Physical Journal C</i> , 2017, 77, 1.	1.4	446
7	Combination of measurements of inclusive deep inelastic $e^\pm p$ scattering cross sections and QCD analysis of HERA data. <i>European Physical Journal C</i> , 2015, 75, 1.	1.4	383
8	Topological cell clustering in the ATLAS calorimeters and its performance in LHC Run 1. <i>European Physical Journal C</i> , 2017, 77, 490.	1.4	325
9	A new evaluation of the hadronic vacuum polarisation contributions to the muon anomalous magnetic moment and to $\alpha(\vec{m})^2$ . <i>European Physical Journal C</i> , 2020, 80, 1.	1.4	318
10	Performance of pile-up mitigation techniques for jets in $pp$ collisions at $\sqrt{s} = 8$ TeV. <i>European Physical Journal C</i> , 2016, 76, 581.	1.4	298
11	Jet energy measurement and its systematic uncertainty in proton-proton collisions at $\sqrt{s} = 7$ TeV with the ATLAS detector. <i>European Physical Journal C</i> , 2015, 75, 17.	1.4	268
12	Updated estimate of the muon magnetic moment using revised results from $e^+e^-$ annihilation. <i>European Physical Journal C</i> , 2003, 31, 503-510.	1.4	263
13	Performance of the ATLAS Trigger System in 2010. <i>European Physical Journal C</i> , 2012, 72, 1.	1.4	259
14	The physics of hadronic tau decays. <i>Reviews of Modern Physics</i> , 2006, 78, 1043-1109.	16.4	214
15	Confronting spectral functions from $ee$ annihilation and $\tau$ decays: consequences for the muon magnetic moment. <i>European Physical Journal C</i> , 2003, 27, 497-521.	1.4	213
16	Measurement of the muon reconstruction performance of the ATLAS detector using 2011 and 2012 LHC proton-proton collision data. <i>European Physical Journal C</i> , 2014, 74, 3130.	1.4	213
17	Performance of missing transverse momentum reconstruction with the ATLAS detector using proton-proton collisions at $\sqrt{s} = 13$ TeV. <i>European Physical Journal C</i> , 2018, 78, 903.	1.4	181
18	The determination of $S$ from $\tilde{l}_\mu$ decays revisited. <i>European Physical Journal C</i> , 2008, 56, 305-322.	1.4	149

#	ARTICLE	IF	CITATIONS
19	Jet reconstruction and performance using particle flow with the ATLAS Detector. European Physical Journal C, 2017, 77, 466.	1.4	145
20	Precision measurement and interpretation of inclusive $W^+W^+$ , $W^-W^-$ . European Physical Journal C, 2017, 77, 367.	1.4	145
21	Update of the ALEPH non-strange spectral functions from hadronic $u\bar{u}$ , decays. European Physical Journal C, 2014, 74, 1.	1.4	140
22	Measurement of the $Z/\tilde{\chi}^0$ boson transverse momentum distribution in pp collisions at $\sqrt{s} = 7$ TeV with the ATLAS detector. Journal of High Energy Physics, 2014, 2014, 1.	1.6	131
23	ATLAS b-jet identification performance and efficiency measurement with $t\bar{t}$ events in pp collisions at $\sqrt{s} = 13$ TeV. European Physical Journal C, 2019, 79, 1.	1.4	130
24	Reevaluation of the hadronic contribution to the muon magnetic anomaly using new $e^+e^- \rightarrow e^+\gamma^*e^- + \text{hadrons}$ cross section data from BABAR. European Physical Journal C, 2010, 66, 1-9.	1.4	128
25	Dark Matter benchmark models for early LHC Run-2 Searches: Report of the ATLAS/CMS Dark Matter Forum. Physics of the Dark Universe, 2020, 27, 100371.	1.8	126
26	Measurements of top-quark pair differential cross-sections in the lepton+jets channel in pp collisions at $\sqrt{s} = 8, 13$ TeV using the ATLAS detector. European Physical Journal C, 2016, 76, 538.	1.4	115
27	The discrepancy between $\tilde{\chi}^0$ , and $e^+e^- \rightarrow e^+\gamma^*e^-$ spectral functions revisited and the consequences for the muon magnetic anomaly. European Physical Journal C, 2010, 66, 127-136.	1.4	110
28	Performance of electron and photon triggers in ATLAS during LHC Run 2. European Physical Journal C, 2020, 80, 1.	1.4	93
29	Muon reconstruction and identification efficiency in ATLAS using the full Run 2 pp collision data set at $\sqrt{s} = 13$ TeV. European Physical Journal C, 2021, 81, 1.	1.4	82
30	Search for dark matter at $\sqrt{s} = 13$ TeV in final states containing an energetic photon and large missing transverse momentum with the ATLAS detector. European Physical Journal C, 2017, 77, 393.	1.4	80
31	Measurement of inclusive $ep$ cross sections at high $Q^2$ at $\sqrt{s} = 225$ and $252$ GeV and of the longitudinal proton structure function $F_L$ at HERA. European Physical Journal C, 2014, 74, 1.	1.4	76
32	Performance of the ATLAS track reconstruction algorithms in dense environments in LHC Run 2. European Physical Journal C, 2017, 77, 673.	1.4	75
33	Measurement of the inclusive and dijet cross-sections of b-jets in pp collisions at $\sqrt{s} = 7$ TeV with the ATLAS detector. European Physical Journal C, 2011, 71, 1.	1.4	73
34	A precision measurement of the inclusive ep scattering cross section at HERA. European Physical Journal C, 2009, 64, 561-587.	1.4	71
35	Reconstruction of primary vertices at the ATLAS experiment in Run 1 proton-proton collisions at the LHC. European Physical Journal C, 2017, 77, 332.	1.4	71
36	Identification and energy calibration of hadronically decaying tau leptons with the ATLAS experiment in pp collisions at $\sqrt{s} = 8$ TeV. European Physical Journal C, 2015, 75, 303.	1.4	70

#	ARTICLE	IF	CITATIONS
37	Jet energy scale and resolution measured in proton-proton collisions at $\sqrt{s}=13$ TeV with the ATLAS detector. European Physical Journal C, 2021, 81, 1.	1.4	64
38	Prompt and non-prompt $J/\psi$ and $\psi(2S)$ suppression at high transverse momentum in $5.02\text{-TeV}$ Pb+Pb collisions with the ATLAS experiment. European Physical Journal C, 2018, 78, 762.	1.4	61
39	Jet production rates in association with W and Z bosons in pp collisions at $\sqrt{s} = 7$ TeV. Journal of High Energy Physics, 2012, 2012, 1.	1.6	58
40	Search for pair production of Higgs bosons in the $b\bar{b}$ final state using proton-proton collisions at $\sqrt{s}=13$ TeV with the ATLAS detector. Journal of High Energy Physics, 2019, 2019, 1.	1.6	55
41	Reconstruction of hadronic decay products of tau leptons with the ATLAS experiment. European Physical Journal C, 2016, 76, 295.	1.4	50
42	Combination and QCD analysis of charm and beauty production cross-section measurements in deep inelastic ep scattering at HERA. European Physical Journal C, 2018, 78, 1.	1.4	49
43	Measurement of the photon identification efficiencies with the ATLAS detector using LHC Run 2 data collected in 2015 and 2016. European Physical Journal C, 2019, 79, 1.	1.4	46
44	Single hadron response measurement and calorimeter jet energy scale uncertainty with the ATLAS detector at the LHC. European Physical Journal C, 2013, 73, 1.	1.4	45
45	Performance of top-quark and W-boson tagging with ATLAS in Run 2 of the LHC. European Physical Journal C, 2019, 79, 1.	1.4	42
46	Measurements of b-jet tagging efficiency with the ATLAS detector using $t\bar{t}$ events at $\sqrt{s}=13$ TeV. Journal of High Energy Physics, 2018, 2018, 1.	1.6	40
47	Electron and photon energy calibration with the ATLAS detector using 2015-2016 LHC proton-proton collision data. Journal of Instrumentation, 2019, 14, P03017-P03017.	0.5	37
48	Search for squarks and gluinos in final states with jets and missing transverse momentum using 139 $\text{fb}^{-1}$ of $\sqrt{s} = 13$ TeV pp collision data with the ATLAS detector. Journal of High Energy Physics, 2021, 2021, 1.	1.6	37
49	Search for a scalar partner of the top quark in the all-hadronic $t\bar{t}$ plus missing transverse momentum final state at $\sqrt{s}=13$ TeV with the ATLAS detector. European Physical Journal C, 2020, 80, 1.	1.4	36
50	Measurement of the inclusive jet cross-section in proton-proton collisions at $\sqrt{s}=7$ TeV using $4.5\text{ fb}^{-1}$ of data with the ATLAS detector. Journal of High Energy Physics, 2015, 2015, 1.	1.6	35
51	Measurement of the cross section for electroweak production of $Z\gamma$ in association with two jets and constraints on anomalous quartic gauge couplings in proton-proton collisions at $\sqrt{s}=13$ TeV. Physics Letters, Section B: Nuclear, Elementary Particle and High Energy Physics, 2017, 778, 368-402.	1.5	34
52	Measurements of top-quark pair differential and double-differential cross-sections in the $t\bar{t}+jets$ channel with pp collisions at $\sqrt{s}=13$ TeV using the ATLAS detector. European Physical Journal C, 2019, 79, 1.	1.4	34
53	Evidence for $t\bar{t}$ production in the multilepton final state in proton-proton collisions at $\sqrt{s}=13$ TeV with the ATLAS detector. European Physical Journal C, 2020, 80, 1.	1.4	30
54	A measurement of the calorimeter response to single hadrons and determination of the jet energy scale uncertainty using LHC Run-1 pp-collision data with the ATLAS detector. European Physical Journal C, 2017, 77, 26.	1.4	29

#	ARTICLE	IF	CITATIONS
55	Measurement of the Drell-Yan triple-differential cross section in pp collisions at $s = 8 \sqrt{s} = 8 \text{ TeV}$ . Journal of High Energy Physics, 2017, 2017, 1.	1.6	28
56	Search for chargino-neutralino pair production in final states with three leptons and missing transverse momentum in $\sqrt{s} = 13 \text{ TeV}$ pp collisions with the ATLAS detector. European Physical Journal C, 2021, 81, 1.	1.4	28
57	Measurement of the cross-section and charge asymmetry of W bosons produced in proton-proton collisions at $\sqrt{s} = 8 \text{ TeV}$ with the ATLAS detector. European Physical Journal C, 2019, 79, 1.	1.4	24
58	Measurement of fiducial and differential $W^+W^-$ production cross-sections at $\sqrt{s} = 13 \text{ TeV}$ with the ATLAS detector. European Physical Journal C, 2019, 79, 1.	1.4	24
59	Measurement of the inclusive jet cross-sections in proton-proton collisions at $s = 8 \sqrt{s} = 8 \text{ TeV}$ with the ATLAS detector. Journal of High Energy Physics, 2017, 2017, 1.	1.6	23
60	Search for doubly and singly charged Higgs bosons decaying into vector bosons in multi-lepton final states with the ATLAS detector using proton-proton collisions at $\sqrt{s} = 13 \text{ TeV}$ . Journal of High Energy Physics, 2021, 2021, 1.	1.6	23
61	AtlFast3: The Next Generation of Fast Simulation in ATLAS. Computing and Software for Big Science, 2022, 6, 1.	1.3	23
62	The performance of the jet trigger for the ATLAS detector during 2011 data taking. European Physical Journal C, 2016, 76, 526.	1.4	21
63	Search for the Standard Model Higgs boson decaying into $b\bar{b}$ produced in association with top quarks decaying hadronically in pp collisions at $s = 8 \sqrt{s} = 8 \text{ TeV}$ with the ATLAS detector. Journal of High Energy Physics, 2016, 2016, 1.	1.6	21
64	Search for new phenomena in final states with b-jets and missing transverse momentum in $\sqrt{s} = 13 \text{ TeV}$ pp collisions with the ATLAS detector. Journal of High Energy Physics, 2021, 2021, 1.	1.6	18
65	Electroweak production of two jets in association with a Z boson in proton-proton collisions at $\sqrt{s} = 13 \text{ TeV}$ . European Physical Journal C, 2018, 78, 1.	1.4	17
66	Measurement of inclusive jet and dijet cross-sections in proton-proton collisions at $\sqrt{s} = 13 \text{ TeV}$ with the ATLAS detector. Journal of High Energy Physics, 2018, 2018, 1.	1.6	17
67	Performance of the missing transverse momentum triggers for the ATLAS detector during Run-2 data taking. Journal of High Energy Physics, 2020, 2020, 1.	1.6	17
68	Search for the $HH \rightarrow b\bar{b}b\bar{b}$ process via vector-boson fusion production using proton-proton collisions at $\sqrt{s} = 13 \text{ TeV}$ with the ATLAS detector. Journal of High Energy Physics, 2020, 2020, 1.	1.6	17
69	Measurement of differential cross sections and $W^+/W^\pm$ cross-section ratios for W boson production in association with jets at $\sqrt{s} = 8 \text{ TeV}$ with the ATLAS detector. Journal of High Energy Physics, 2018, 2018, 1.	1.6	16
70	Optimisation of large-radius jet reconstruction for the ATLAS detector in $13 \text{ TeV}$ proton-proton collisions. European Physical Journal C, 2021, 81, 1.	1.4	15
71	Determination of jet calibration and energy resolution in proton-proton collisions at $\sqrt{s} = 8 \text{ TeV}$ using the ATLAS detector. European Physical Journal C, 2020, 80, 1.	1.4	15
72	Measurements of Higgs bosons decaying to bottom quarks from vector boson fusion production with the ATLAS experiment at $\sqrt{s} = 13 \text{ TeV}$ . European Physical Journal C, 2021, 81, 1.	1.4	14

#	ARTICLE	IF	CITATIONS
73	Measurement of the c-jet mistagging efficiency in $t\bar{t}$ events using pp collision data at $\sqrt{s} = 13$ TeV collected with the ATLAS detector. European Physical Journal C, 2022, 82, .	1.4	14
74	Search for long-lived particles decaying to leptons with large impact parameter in proton-proton collisions at $\sqrt{s} = 13$ TeV. European Physical Journal C, 2022, 82, 153.	1.4	14
75	Search for dark photons in decays of Higgs bosons produced in association with Z bosons in proton-proton collisions at $\sqrt{s} = 13$ TeV. Journal of High Energy Physics, 2019, 2019, 1.	1.6	13
76	Search for dark matter in events with missing transverse momentum and a Higgs boson decaying into two photons in pp collisions at $\sqrt{s} = 13$ TeV with the ATLAS detector. Journal of High Energy Physics, 2021, 2021, 1.	1.6	12
77	Alignment of the ATLAS Inner Detector in Run 2. European Physical Journal C, 2020, 80, 1.	1.4	12
78	Determination of the parton distribution functions of the proton using diverse ATLAS data from pp collisions at $\sqrt{s} = 7, 8$ and 13 TeV. European Physical Journal C, 2022, 82, 1.	1.4	12
79	Determination of the parton distribution functions of the proton from ATLAS measurements of differential $W^{\pm}$ and Z boson production in association with jets. Journal of High Energy Physics, 2021, 2021, 1.	1.6	10
80	Measurement of the $t\bar{t}$ production cross section in pp collisions at $\sqrt{s} = 13$ TeV with the ATLAS detector. Journal of High Energy Physics, 2021, 2021, 1.	1.6	10
81	Search for Higgs bosons decaying into new spin-0 or spin-1 particles in four-lepton final states with the ATLAS detector with $139 \text{ fb}^{-1}$ of pp collision data at $\sqrt{s} = 13$ TeV. Journal of High Energy Physics, 2022, 2022, 1.	1.6	10
82	Search for dark matter produced in association with a Standard Model Higgs boson decaying into b-quarks using the full Run 2 dataset from the ATLAS detector. Journal of High Energy Physics, 2021, 2021, 1.	1.6	10
83	Measurement of the inclusive cross-section for the production of jets in association with a Z boson in proton-proton collisions at 8 TeV using the ATLAS detector. European Physical Journal C, 2019, 79, 1.	1.4	9
84	Review of Recent Calculations of the Hadronic Vacuum Polarisation Contribution. EPJ Web of Conferences, 2016, 118, 01036.	0.1	8
85	Measurements of $W+W^{\pm} + \geq 1$ jet production cross-sections in pp collisions at $\sqrt{s} = 13$ TeV with the ATLAS detector. Journal of High Energy Physics, 2021, 2021, 1.	1.6	8
86	Observation of electroweak production of two jets in association with an isolated photon and missing transverse momentum, and search for a Higgs boson decaying into invisible particles at $\sqrt{s} = 13$ TeV with the ATLAS detector. European Physical Journal C, 2022, 82, 1.	1.4	8
87	Search for R-parity-violating supersymmetry in a final state containing leptons and many jets with the ATLAS experiment using $\sqrt{s} = 13$ TeV proton-proton collision data. European Physical Journal C, 2021, 81, 1.	1.4	7
88	Configuration and performance of the ATLAS b-jet triggers in Run 2. European Physical Journal C, 2021, 81, 1.	1.4	7
89	Search for flavour-changing neutral-current interactions of a top quark and a gluon in pp collisions at $\sqrt{s} = 13$ TeV with the ATLAS detector. European Physical Journal C, 2022, 82, .	1.4	7
90	Measurement of the ratio of cross sections for inclusive isolated-photon production in pp collisions at $\sqrt{s} = 13$ and 8 TeV with the ATLAS detector. Journal of High Energy Physics, 2019, 2019, 1.	1.6	6

#	ARTICLE	IF	CITATIONS
91	Search for Higgs boson production in association with a high-energy photon via vector-boson fusion with decay into bottom quark pairs at $\sqrt{s} = 13$ TeV with the ATLAS detector. Journal of High Energy Physics, 2021, 2021, 1.	1.6	6
92	Performance of the ATLAS Level-1 topological trigger in Run 2. European Physical Journal C, 2022, 82, 1.	1.4	6
93	Extraction of top backgrounds in the Higgs boson search with the $H \rightarrow WW(\ast) \rightarrow a, \bar{a}, \tau, \bar{\tau} + E_{\text{miss}}$ decay with a full-jet veto at the LHC. Physical Review D, 2011, 84, .	1.6	5
94	A search for the decays of stopped long-lived particles at $\sqrt{s} = 13$ TeV with the ATLAS detector. Journal of High Energy Physics, 2021, 2021, 1.	1.6	5
95	The ATLAS inner detector trigger performance in pp collisions at 13 TeV during LHC Run 2. European Physical Journal C, 2022, 82, 1.	1.4	5
96	Measurement of the energy response of the ATLAS calorimeter to charged pions from $W \rightarrow \mu \nu$ events in Run 2 data. European Physical Journal C, 2022, 82, 1.	1.4	4
97	Measurement of the production cross section of pairs of isolated photons in pp collisions at 13 TeV with the ATLAS detector. Journal of High Energy Physics, 2021, 2021, 1.	1.6	4
98	Search for exotic decays of the Higgs boson into long-lived particles in pp collisions at $\sqrt{s} = 13$ TeV using displaced vertices in the ATLAS inner detector. Journal of High Energy Physics, 2021, 2021, 1.	1.6	4
99	Measurement of the inclusive jet cross-section in proton-proton collisions at ( $\sqrt{s}=7$ ) TeV using 4.5 fb <sup>-1</sup> of data with the ATLAS detector. , 2015, 2015, 1.		3
100	Measurement of b-quark fragmentation properties in jets using the decay $B \rightarrow \tau^+ J/\psi K^{\pm}$ in pp collisions at $\sqrt{s} = 13$ TeV with the ATLAS detector. Journal of High Energy Physics, 2021, 2021, 1.	1.6	3
101	Search for exotic decays of the Higgs boson into $b\bar{b}$ and missing transverse momentum in pp collisions at $\sqrt{s} = 13$ TeV with the ATLAS detector. Journal of High Energy Physics, 2022, 2022, 1.	1.6	2
102	Measurement of the energy asymmetry in $t\bar{t}$ production at $\sqrt{s}=13$ TeV with the ATLAS experiment and interpretation in the SMEFT framework. European Physical Journal C, 2022, 82, .	1.4	2
103	Status of Leading-Order Hadronic Vacuum Polarization Dispersion Calculation. Nuclear Physics, Section B, Proceedings Supplements, 2014, 253-255, 131-134.	0.5	1
104	Reevaluation of the hadronic contributions to the muon $g-2$ and to $(\alpha(M_Z^2))$ . , 2011, 71, 1.		1
105	Detector and trigger challenge for supersymmetrical dark matter scenarios at the international linear collider. Pramana - Journal of Physics, 2007, 69, 1195-1198.	0.9	0
106	$\tau$ Decays and $\langle m_{\mu} \rangle$  overflow="scroll" xmlns:xocs="http://www.elsevier.com/xml/xocs/dtd" xmlns:xs="http://www.w3.org/2001/XMLSchema" xmlns:xsi="http://www.w3.org/2001/XMLSchema-instance" xmlns="http://www.elsevier.com/xml/ja/dtd" xmlns:ja="http://www.elsevier.com/xml/ja/dtd" xmlns:mml="http://www.w3.org/1998/Math/MathML" xmlns:tb="http://www.elsevier.com/xml/common/table/dtd" xmlns:sb="http://www.elsevier.com/xml/common/struct-bib/dtd" xmlns:ce="http://www.elsevier.com/x	0.2	0